Scientific Research Publishing

International Journal of Geosciences, 2024, 15, 231-245
https://www.scirp.org/journal/ijg
ISSN Online: 2156-8367
ISSN Print: 2156-8359

Structural Controls Analysis and Its Correlation with Geothermal Occurrence at Barrier Volcanic Complex (BVC), Turkana, Kenya

Philip Lomorukai Emekwi, Nicholas O. Mariita, Patrick Chege Kariuki

Geothermal Training and Research Institute (GeTRI), Dedan Kimathi University of Technology, Nyeri, Kenya
Email: lomorukaiphilip@gmail.com, nicholas.mariita@dkut.ac.ke, patrick.kariuki@dkut.ac.ke

How to cite this paper: Emekwi, P.L., Mariita, N.O. and Kariuki, P.C. (2024) Structural Controls Analysis and Its Correlation with Geothermal Occurrence at Barrier Volcanic Complex (BVC), Turkana, Kenya. *International Journal of Geosciences*, **15**, 231-245.
https://doi.org/10.4236/ijg.2024.153014

Received: January 11, 2024
Accepted: March 22, 2024
Published: March 25, 2024

Abstract

Geothermal is a clean energy source that is freely available in the subsurface. The exploitation of this vital resource needs intensive exploration in order to identify and quantify its occurrence. The three parameters considered when assessing the viability of a geothermal system include; heat source, fractures and fluids. Geological structures are important in transportation of fluids to and from the heat source aiding in recharge of the geothermal system and enhancing productivity. Remote sensing method was applied in mapping the structures at Barrier Volcanic Complex (BVC) by using hill shading technique which utilized four illumination angles of the sun (azimuth) *i.e.* 45˚, 90˚, 150˚, and 315˚, constant elevation of 45˚ and exaggeration of 10. The data used was Shuttle Radar Topographic Mission (SRTM) Satellite Imagery. ArcGIS Software was used for lineaments delineation and density mapping, PCI Geomatica was used to generate major faults, while Georose and Rockworks 17 were used to generate the rose diagrams. Geological structural analysis was done by delineating lineaments, determining the density distribution of lineaments and finally determining the structural trends of lineaments. The generated major faults in the area and the location of the occurrence of surface manifestations were compared with the generated lineaments. A total of 260 lineaments were generated whereby at 45˚ there was a total of 60 lineaments, at 90˚ 95 lineaments, at 150˚ 61 lineaments, and at 315˚ 44 lineaments. The results of structural analysis in the area as shown by the rose diagrams indicate an NNE-SSW and N-S trending of structures. In conclusion, the study area is highly fractured as indicated by the presence of numerous lineaments. These lineaments provide good recharge to the geothermal system and enhance the geothermal reservoir in the area.

Keywords

Geothermal Resource, Lineaments, Lineaments Density,

Structural Controls

1. Introduction

Barrier Volcanic Complex (BVC) is a geothermal prospect situated at Turkana, along the East African Rift System (EARS) specifically the Kenyan rift. It is 20 km in length and 15 km wide, and forms a natural dam across the inner trough separating Lake Turkana from Suguta Valley. The prospect covers an area of 380 km^2. Geographically, it is located at coordinates 2.3192˚N, 36.5879˚E (Figure 1).

BVC is a composite structure that is made up of four separate volcanic centers. These centers include Barrier, Kalolenyang, Kakorinya, and Likau (Figure 2). They are made up of different kinds of lava, namely; basanite, basalt, hawaiite, mugearite, benmorite, trachyte, and phonolite, among others. Kakorinya is the youngest of the volcanic centers. Dindi (2020) reported that the Kenyan rift is an active system with volcanic activities taking place hence surface geothermal manifestations like hot springs, geysers, fumaroles, altered grounds, occurrence at the rift zone [1]. This is evident in BVC through occurrence of

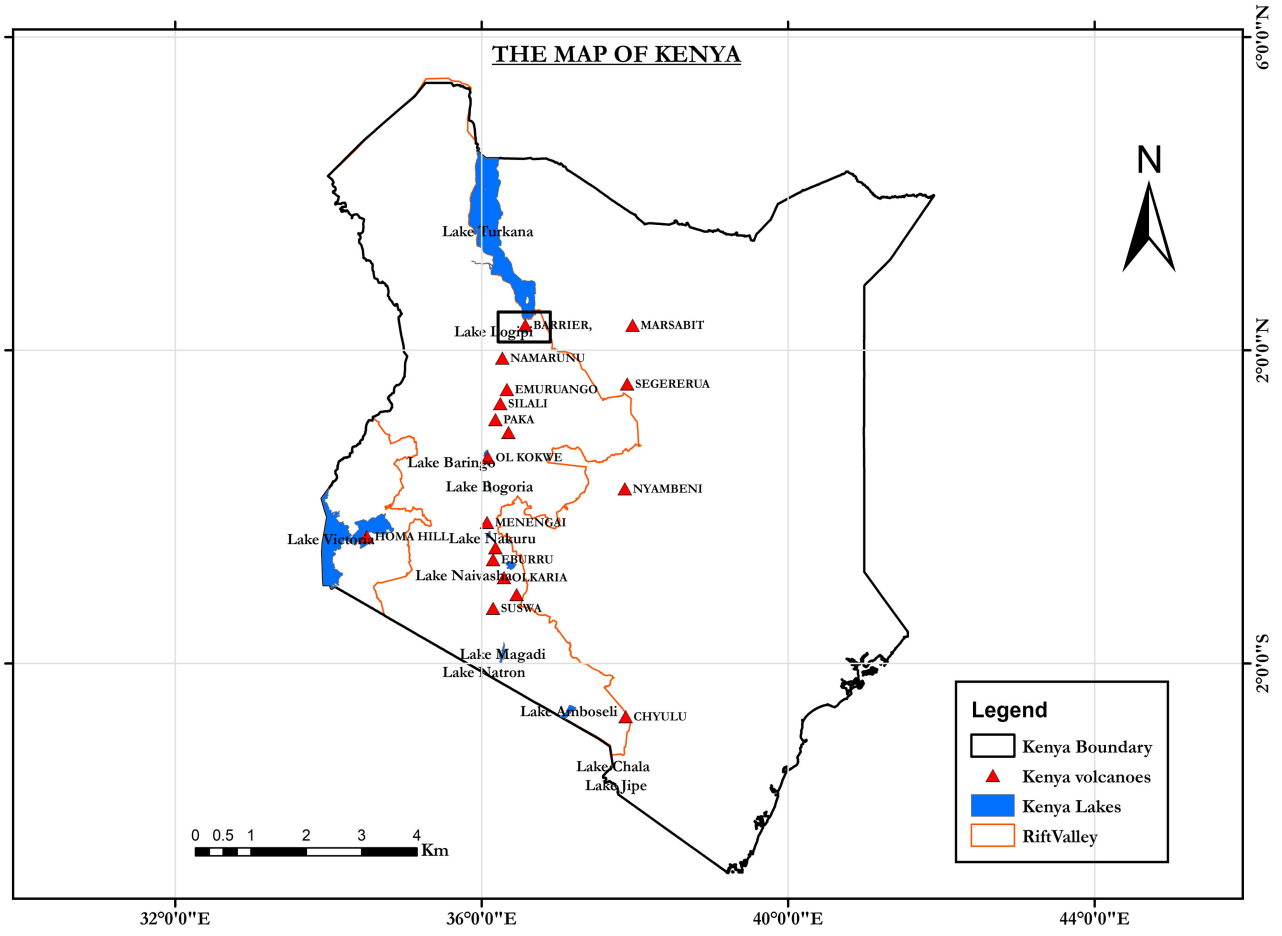

Figure 1. Map of the Kenya showing the location of Barrier Volcanic complex in the rift.

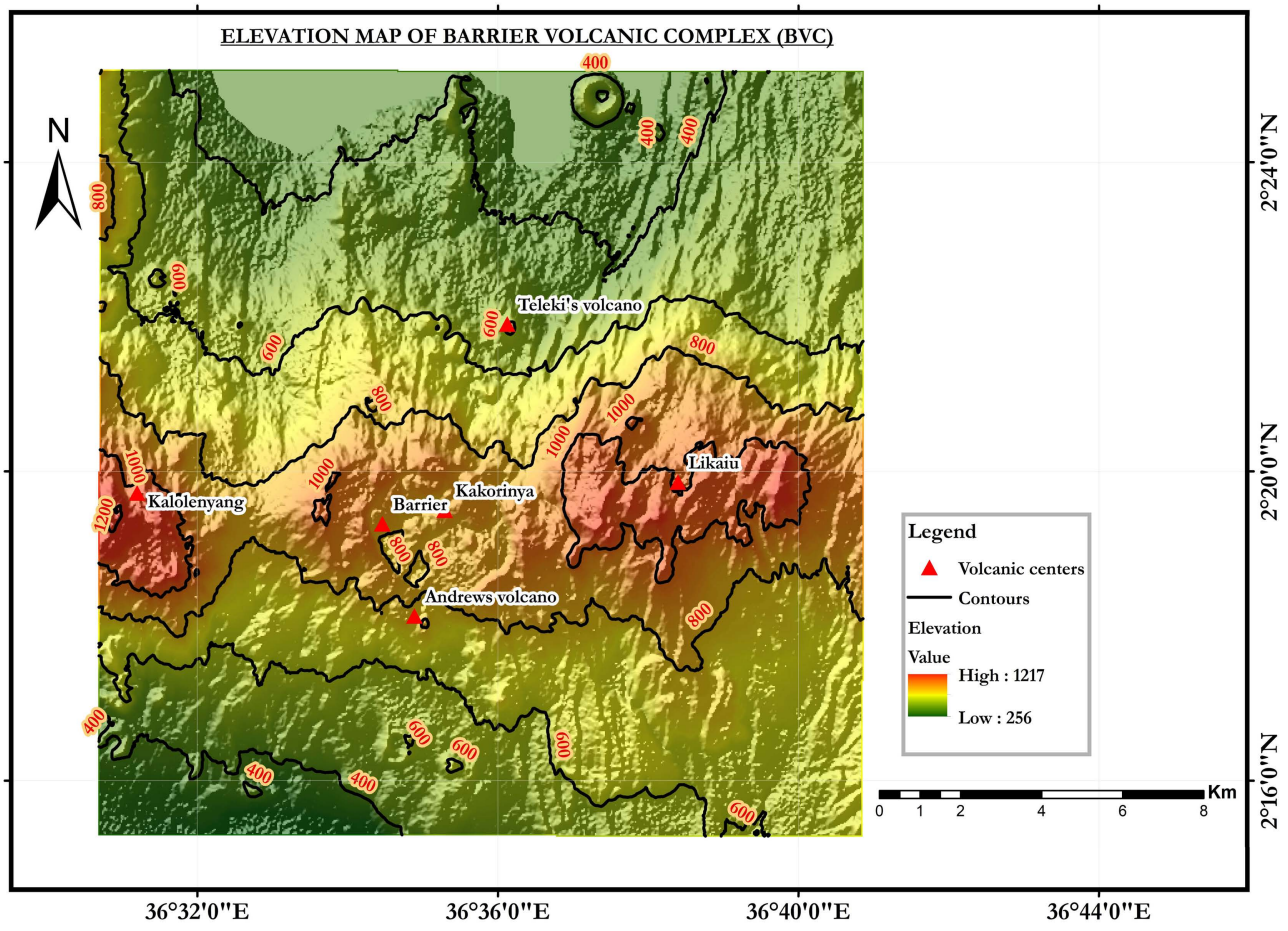

Figure 2. Elevation map of barrier volcanic complex as a study area with volcanic centers.

fumaroles and the upper western and southern flanks of the caldera having hot hydrothermally altered grounds. A number of sites on the rim of the caldera have silica veins and sinters, both of which are indicators of the presence of active hot springs in the past.

Synoptic view in remote sensing enables enhanced visualization and better understanding of the relation between the whole terrain of an area and its features [2]. Several studies have demonstrated the effectiveness of remote sensing techniques for identifying the structural controls. Hamimi *et al.*, 2020 applied remote sensing technique in mapping geological structures at Atalla Shear Zone and Environs, Central Eastern Desert, Egypt where band rationing was performed for Landsat images for the true and false color composites which revealed the NE to NNE orientation of the structures in the study area [3].

Skakni *et al.* (2022) used an integrated Geographic Information System (GIS), Remote Sensing and resistivity approach to conduct a structural mapping of initially inaccessible zones in the North-Western Rift Belt in Morocco [4]. The study combined Principal Component Analysis, directional filtering, and Optimal Index Factor to generate images for mapping the lithology of the zone.

Due to active tectonic setting of a prospect such as BVC, remote sensing ap-

proach is essential in order to detect morphological changes by identifying the significant difference between the multi-temporal Landsat images [5] and the elevation changes using Shuttle Radar Topography Mission (SRTM). Field mapping of lineaments is expensive and time consuming, hence use of remote sensing has been widely applied [5] in lineaments delineation.

Geothermal Development Company (GDC) of Kenya did geoscientific studies (geophysics, geology and geochemistry) in 2011 to ascertain the potential of geothermal resource in the study area. They found that the area has a potential of about 700 MWe for electrical generation. Since the potential of the study area was estimated by GDC, there was need to study the structural controls that act as conduits to recharging the geothermal system in the area. This therefore, prompted the application of remote sensing technique in this research to map and analyze the structural controls at Barrier Volcanic complex (BVC). This is because understanding fracture distribution is crucial in siting of exploratory wells, reservoir management, as well as ensuring sustainable geothermal resource production. Presence of water is important to the future exploitation of the geothermal resource in the area to avoid drilling of tight wells. All these needs necessitated the application of remote sensing satellite imagery and Shuttle Radar Topography Mission (SRTM) in mapping of structural controls in the study area since it has been applied in many geothermal fields for exploration and exploitation expansive purposes.

2. Geological Setting

2.1. Tectonic and Geological Setting

BVC is located in the Turkana rift zone which is within the Kenyan Rift system. The Kenya Rift is comprised of both the Turkana Rift Zone and the Kenya Rift Zone [6]. It generally follows the boundary between the Proterozoic Mozambique Belt and the Archean Tanzania Craton [7]. The northern, central, and southern segment of the Kenya Rift have half graben geometries due to earlier faulting and pronounced subsidence along the western boundary faults [6]. For most of the structural evolution of the Kenya Rift, faulting has been controlled by an E-W oriented position of minimum stress [8].

Volcanic activity in Turkana rift, which was followed by activity moving southwards, was the initial step in the formation of the Kenya rift during the early Miocene (14 - 23 Ma BP). Faulting that occurred in conjunction with rifting took place in many stages, beginning with faulting on the western side, which was accompanied by basaltic and phonolitic volcanism on the crust of the uplift [9]. Major faults extended along the western side, generating a half graben that was bordered on the eastern side by a monoclinic flexure. At the same time, the development of massive basaltic-trachytic shield volcanoes was taking place. On the eastern side, major faults formed, which resulted in the transformation of the half graben into a complete graben and was followed by basalt-trachyte volcanism.

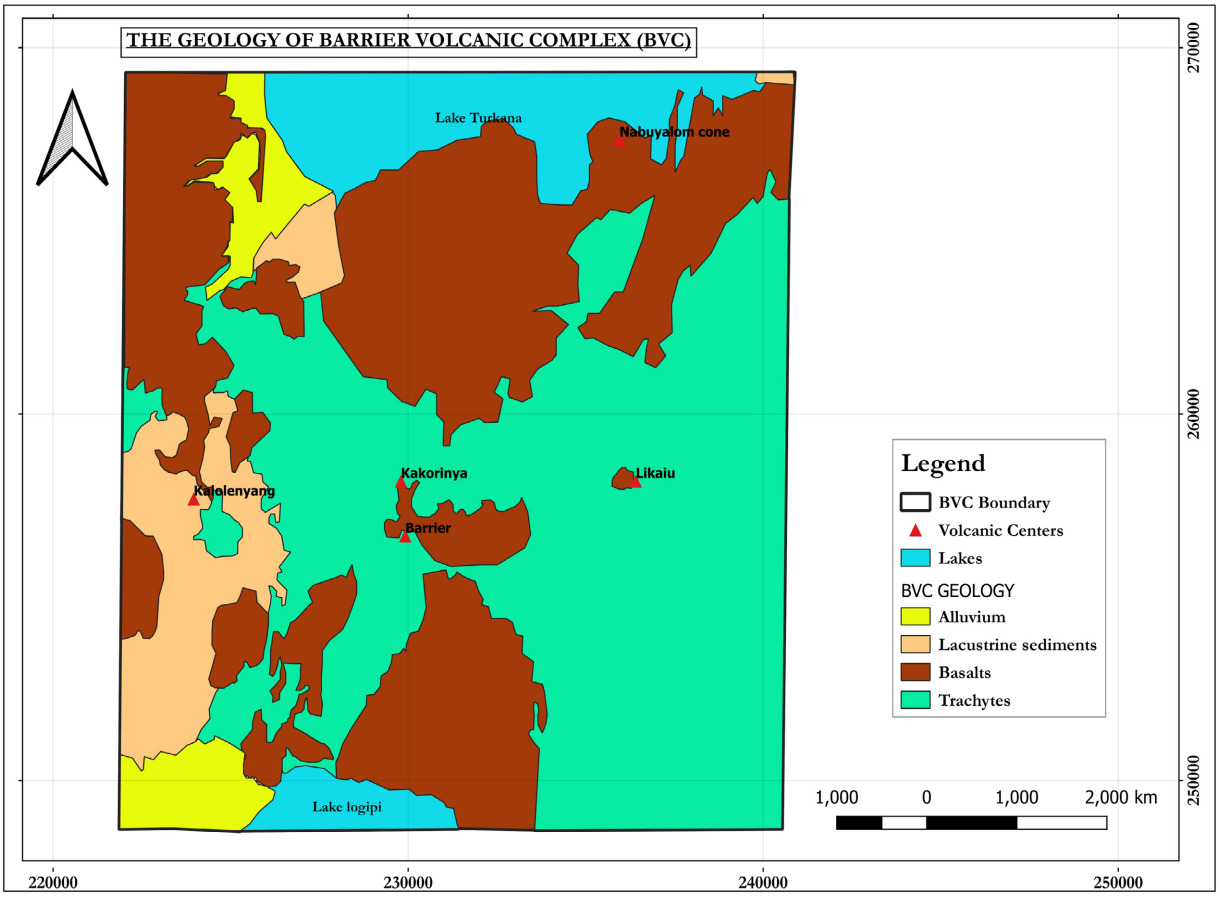

Figure 3. Simplified geological map of the barrier volcanic complex.

Around 5 million years ago (Miocene epoch), the graben structure began to take shape. Subsequently, fissure eruptions in the axis of the rift led to the creation of flood lavas between 2 and 1 million years ago (Quaternary period). Within the axis of the rift, volcanic activity has been growing increasingly intense over the past two million years. Large Quaternary shield volcanoes, notably the Barrier Volcanic Complex, began to form along the Kenya rift axis during this time period. The majority of these volcanoes are geothermal potential areas.

2.2. Stratigraphy

Volcanism in BVC commenced with the eruption of strongly undersaturated flood basalts from a series of fissures along the eastern margin of the trough. Trachyte volcanism commenced with the eruption of lavas and pyroclastic flows from Likaiu East and Kalolenyang volcanoes in the period extending from at least 1.3 Ma to 0.7 Ma [10]. These eruptions build up steep sided edifices, the summit of which later collapsed to form craters. Small volumes of basalts were erupted at a late stage. Rejuvenation of rift margin structures faulted and tilted this center before the next phase of activity.

Likau West (0.5 - 0.2 Ma) is poorly exposed. The summit area is covered by

small trachyte and phonolite lava domes and associated pyroclastic deposits. Volcanism on the BVC culminated with the formation of Kakorinya volcano (>0.2 Ma to Recent). The construction of the lava shield was accompanied by the eruption of extensive pyroclastic flow deposit and air-fall tuff on the western flanks of the volcano. Collapse of the summit area of Kakorinya took place in two stages. Two outer ring faults formed immediately after the Upper trachytes were erupted and were associated with limited basaltic activity on the summit area (**Figure 3**). These fractures are post-dated by trachyte lava domes and widespread air-fall tuffs, the eruption of which triggered the formation of the caldera at 92 ka [10], as shown in **Table 1**.

Table 1 below shows the generalized stratigraphy of the Barrier Volcanic Complex.

Table 1. Stratigraphy of Barrier Volcanic Complex (BVC) as constructed by [10].

	KAKORINYA VOLCANO	
	Recent Basalts and Mugearites (K^{by}, K^{my})	1 Ka - 1921
	Recent Phonolites (K^{py})	
	Upper Basalts (K^{bu})	
	Trachyte lavas and domes (K^{t})	58 ± 4 ka
	CALDERA FORMATION AND FAULTING	
1.	Pyroclastic deposits (K^{vu})	92 ± 2 Ka
	Trachyte lava domes (K^{td})	
	RING FRACTURE AND FAULTING	
	Lower Basalts (K^{bl})	
	Lower Trachytes (K^{tu}) including pyroclastic deposits	221 ± 4 - 97 ± 3 Ka
	Lower Trachytes (K^{tl}) including pyroclastic deposits	
	Faulting	
	LIKAIU WEST VOLCANO	
	Hawaiite lavas (LW^{h}) and Basalt lavas (LW^{b})	
2.	Trachyte and phonolitic pyroclastic flow and breccia deposits (LW^{tv})	
	Basalts of Namurinyang tuff cone (N^{b})	
	FAULTING	
	KALOLENYANG VOLCANO	
3.	Mugearite lavas (KLm)	
	Basalt lavas (KLb)	
	Trachyte lavas (KLt) and pyroclastic flow deposits	773 ± 7 - 707 ± 6 Ka
	LIKAIU EAST	
4.	Trachyte lavas (Let) and pyroclastic flow deposits	1.37 - 1.34 Ma
	FOUNDATION ROCKS	
	Basalt lavas of Logipi and Latarr (B^{b})	

3. Materials and Methods

3.1. Shuttle Radar Topography Mission (SRTM) Data

The digital elevation SRTM data was downloaded from Earth Explorer USGS website. The period of the data was 01-01-2000 to 31-12-2020, a range of 20 years. The image with less atmospheric noise was selected and downloaded for processing and analysis using the WGS-84 datum, and 37N UTM zone map projection. The study area was clipped out using the BVC shapefile. The clipped image was double-blurred to smooth it for clear geological structural identity.

PCI Geomatica was used for generating major geological structures in the area. The digital elevation model of BVC was imported into the software, run it, and the results was generated in terms of a shapefile of major geological structures *i.e.* faults in the area. ArcGIS was used for drawing the lineaments and generating a structural density map. The lineaments generated from ArcGIS were exported into Rockworks 17 in form of file for generation of a rose diagram.

The geological structural analysis was done in three steps namely; delineation of lineaments, determination of lineaments density and finally determination of major trends of lineaments. The results of the analyses gave a clear map on the trend of structures that influence the geothermal system in the study area. The steps used are further discussed in the proceeding text.

3.1.1. Delineation of Lineaments

Lineaments are surface manifestations of structurally controlled features, such as joints, straight course of streams and vegetation alignments [11]. Hill-shading technique was used in delineation of structures. This technique recognizes the use of Digital elevation model (DEM) to generate lineaments by producing a map with different shades of gray [12]. Hill shading map shows the terrain representation and geomorphological tilting [13]. The technique has been applied by map users in many fields including Geographic Information Systems (GIS), cartography, and 3D terrain visualization.

The aim was to map all the possible lineaments that can be recognized on the SRTM Satellite Imagery in the study area by utilizing four illumination directions of 45˚, 90˚, 150˚, and 315˚, a constant elevation of 45˚ and exaggeration of 10. ArcGIS was used in applying this concept.

3.1.2. Determination of Lineaments Density

This stage provides the concentration of lineaments delineated from the previous step. The frequency of the lineaments per unit area (pixel) that will result in a lineament density map was determined at this stage. In each pixel grid, the grid sections were measured in length. The calculation's outcome is then represented by a middle point in the middle of each grid. The output of the representation was contours that display the significant amount of obtained contour based on the concentration of lineaments.

3.1.3. Determination of Major Trends of Lineaments

Major trends were determined by use of lineament densities. All delineation step

results are collated, and Rose diagrams were created to determine the main direction of the lineaments produced. Major trends show the regional flow of fluids and the occurrence of geothermal resource. The results can be supported by the sites/locations of surface manifestations within the study area.

3.2. Ground Truthing

The GPS was used for collecting coordinates of the structures mapped on-site. The Branton Compass was used for recording the strikes and dips, see Table 2. The data on the location of hot springs and fumaroles was obtained from Ol Suswa Energy Limited which has been licensed to explore the geothermal resource in BVC. The raw data on strikes and dips was input into the Georose Software and the results were the generation of a Rose diagram. Figure 13 shows the distribution and location of the mapped structures.

4. Results and Discussion

4.1. Lineaments Delineation

The total number of lineaments generated in the study area were 260; whereby at an azimuth of 45˚ a total of 60 lineaments, at 90˚ was 95 lineaments, at 150˚ was 61, and at 315˚ was 44 lineaments were generated. The lineaments generated for different Azimuths are shown in Figures 4-7. The results were compiled into one map as represented in Figure 8.

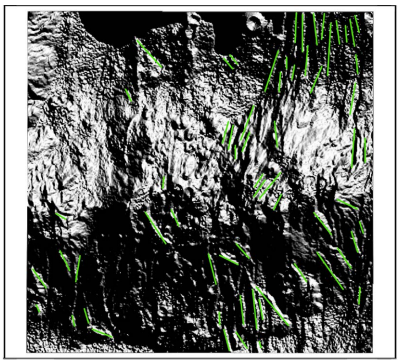

Figure 4. Azimuth of 45˚, 45˚ elevation, exaggeration of 10.

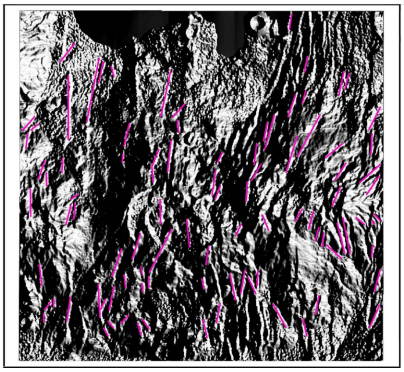

Figure 5. Azimuth of 90˚, 45˚ elevation, exaggeration of 10.

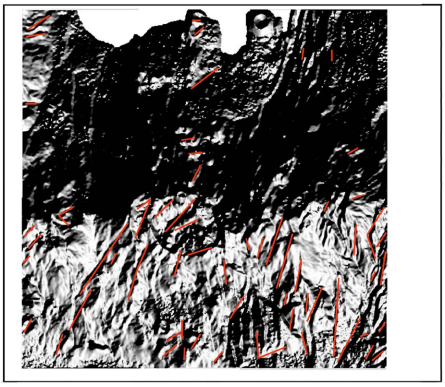

Figure 6. Azimuth of 150˚, 45˚ elevation, exaggeration of 10.

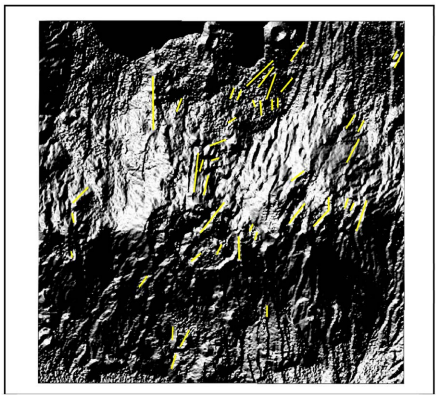

Figure 7. Azimuth of 315˚, 45˚ elevation, exaggeration of 10.

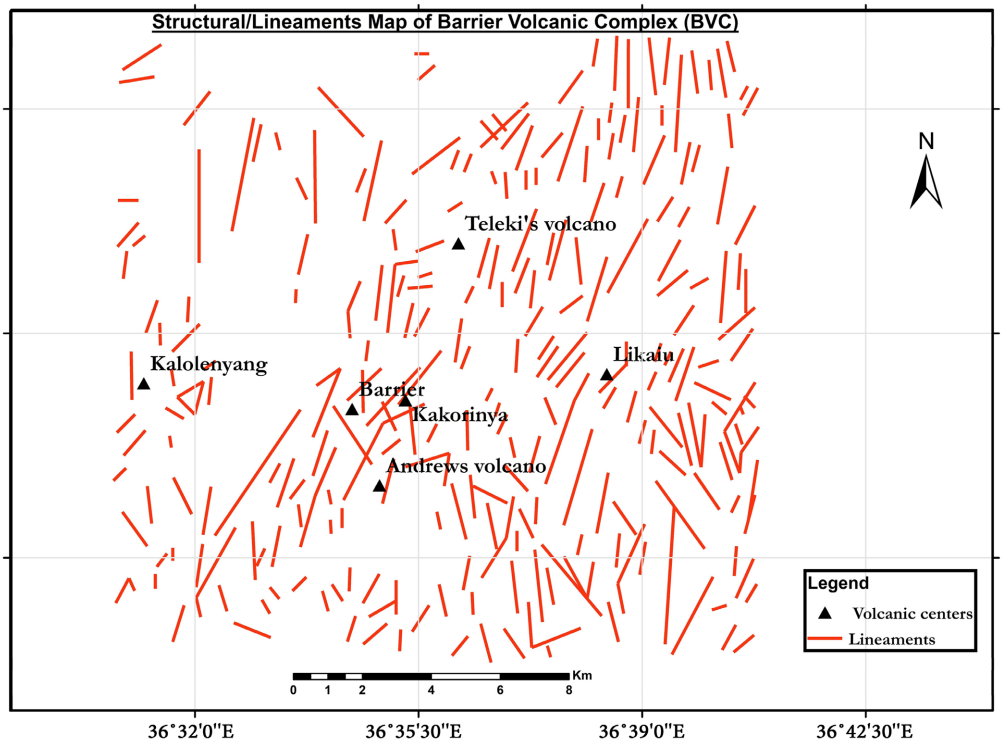

Figure 8. Lineaments map of Barrier Volcanic Complex (BVC).

The hot springs in the southern part of the area occurring in the East-West direction are evident with results generated by PCI Geomatica but not evident with ArcGIS drawn lineaments. It is also evident that the geothermal manifestations *i.e.*, hot springs and fumaroles (Figure 9) in the area occur along the delineated geological structures. The E-W occurring structures indicated by hot springs can be as a result of folding.

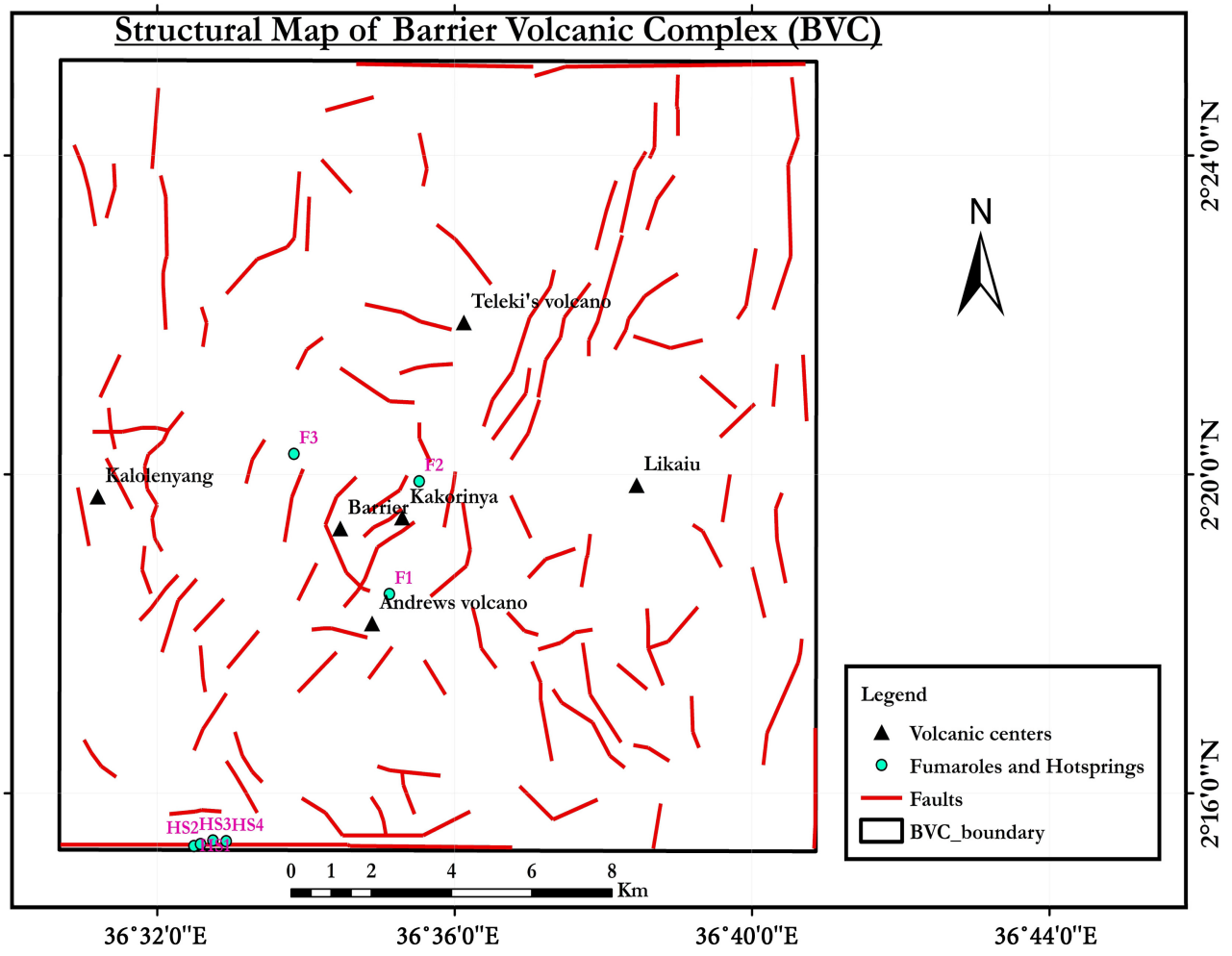

Figure 9. Major geological structures in the area, generated from PCI Geomatica.

4.2. Lineaments Density

For analysis and construction of lineaments density map the lineaments shown in Figure 8 were used. From the color ramp of Figure 10, the highest density areas are represented in red while low density areas are represented in green, and lowest/no lineament areas are in white color. From the results, there is localised high concentration of lineaments in the four volcanic centers which shows high potential for occurrence of geothermal resource. However, there could be an impermeable layer that separates Kalolenyang to the western part of the area with the other three volcanic centers hence having a separate geothermal system with distinct recharge.

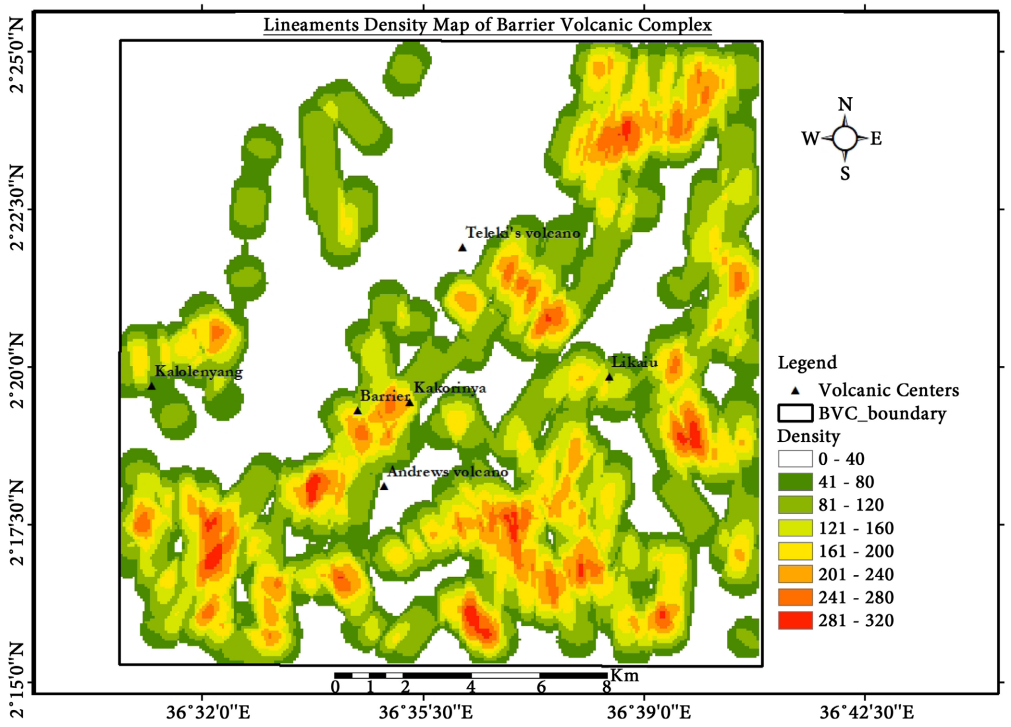

Figure 10. Lineaments density map.

4.3. Determination of Major Trends

The results from the two previous steps were used to determine the major trends in the study area. The delineated lineaments were compiled and processed to generate a Rose diagram that shows the dominant orientation of the lineaments as shown in **Figure 11**.

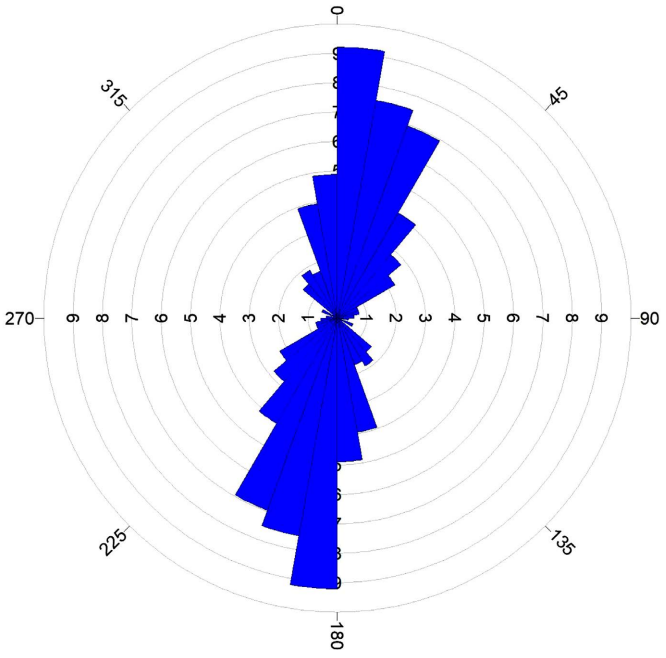

Figure 11. Rose diagram generated from delineated lineaments.

From Figure 11, the geological structures at BVC are trending in the NNE-SSW, and N-S. These trends of geological structures might have been as a result of faulting towards the east as reported by (10). The North-South trending is associated with the North trending normal faulting at the rift margin that led to the formation of the inner trough of BVC as well basalts of Logipi.

4.4. Ground Truthing

To ensure the accuracy of the data, ground truthing was necessary for the calibration and validation of remote sensing models. This increased the precision and reliability of the analysis and result in more informed decision-making processes by cross-referencing data from remote sensing with information from the ground (See Figure 12). Ground truthing was done by measuring the strikes and dips at BVC in order to confirm the major trends (See Table 2). The raw data on strikes and dips was input into the Georose Software and the results were the generation of a Rose diagram shown in Figure 13.

This involved collection of on-site data to enhance the accuracy of data obtained remotely and was done by visiting the study area and taking measurements of strikes and dips, coordinates of the mapped structures, and general ground topography (Table 3). 12 accessible structures in the area were mapped and the result was a generation of a rose diagram shown in Figure 13. The trend of structures is in the NE-SW direction which supports the structural trends in Figure 11. This validated the reliability and legitimacy of information extracted from satellite imagery.

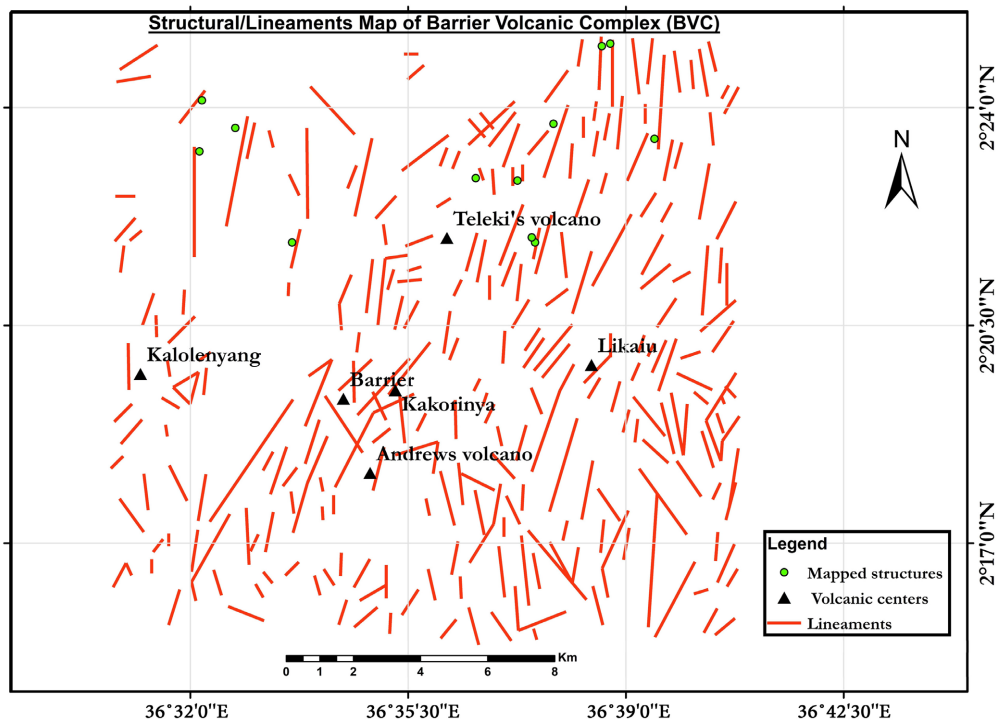

Figure 12. Map showing the mapped structures at BVC during ground truthing.

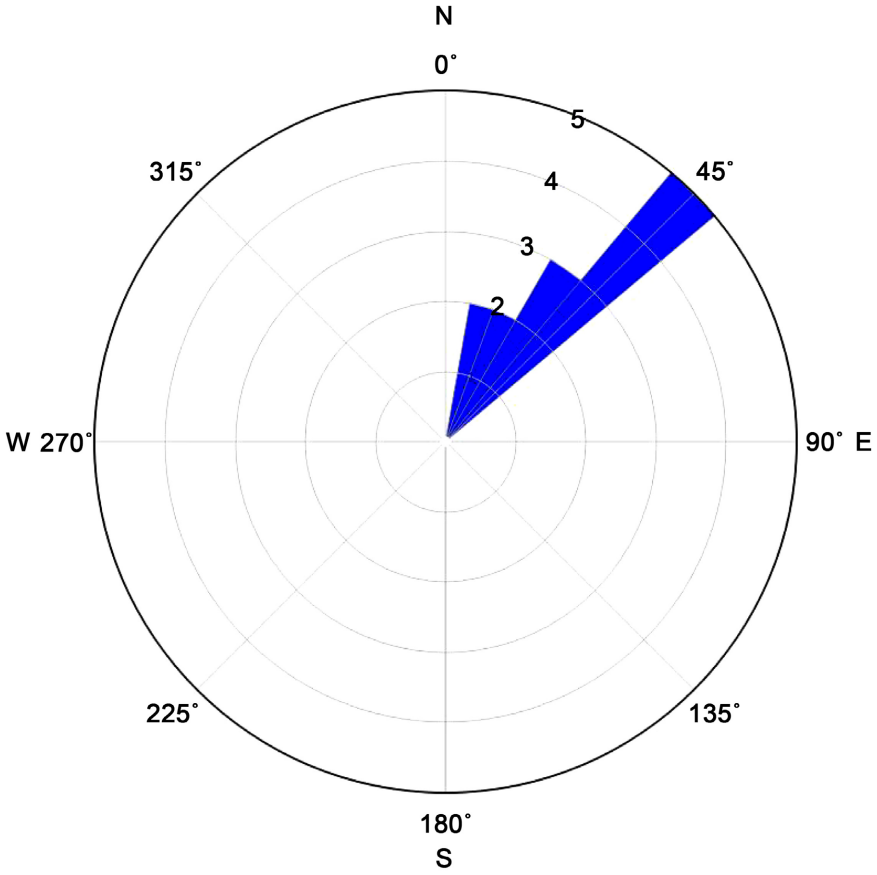

Figure 13. Rose diagram generated from ground truthing data.

Table 2. Location data for mapped structures at BVC.

Mapped structures at Barrier volcanic complex				
S/NO	Strike angle	Dip angle	Coordinates	
			Longitudes	Latitudes
1.	310	40	36.630609	2.395663
2.	285	15	36.557031	2.391862
3.	305	35	36.657670	2.391638
4.	315	45	36.643581	2.416462
5.	312	42	36.545401	2.394545
6.	317	47	36.609811	2.381127
7.	292	22	36.620993	2.380456
8.	280	10	36.535785	2.388283
9.	294	24	36.624795	2.365248
10.	300	30	36.560609	2.363906
11.	302	32	36.645817	2.417133
12.	310	40	36.536455	2.401926

Table 3. Coordinates of fumaroles and hot springs at BVC.

Station Name	Coordinates	
	Longitudes	Latitudes
F1	36.58538	2.308319
F2	36.592061	2.331877
F3	36.563979	2.337632
HS1	36.541564	2.255656
HS2	36.543037	2.256074
HS3	36.545795	2.256811
HS4	36.548778	2.256653

5. Conclusion

The study shows good distribution of lineaments with major trends occurring in the NNE-SSW, and N-S, hence presumed to have been influenced by the east faulting in the area. This is supported by the high density of lineaments in the same direction. Geothermal surface manifestations in the area, fumaroles and hot springs, occur in the NE-SW & E-W direction along the mapped lineaments/faults, which can be used as an effective observatory method for exploring and locating possible drilling locations in future exploitation of geothermal resource in the area.

Conflicts of Interest

The authors declare no conflicts of interest regarding the publication of this paper.

References

[1] Dindi, E.W. (2020) Kenya Rift Valley: Tectonics, Natural Resources, Hazards and Hazard Mitigation. 3*rd Annual Science for Sustainable Development Conference*, 14-16 October 2020, Nairobi, 1-22.

[2] Mather, P.M. and Koch, M. (2011) Front Matter. *Computer Processing of Remotely-Sensed Images*. John Wiley & Sons, Ltd., New York, i-xxv.

[3] Hamimi, Z., Hagag, W., Kamh, S. and El-Araby, A. (2020) Application of Remote-Sensing Techniques in Geological and Structural Mapping of Atalla Shear Zone and Environs, Central Eastern Desert, Egypt. *Arabian Journal of Geosciences*, **13**, 414. https://doi.org/10.1007/s12517-020-05324-8

[4] Skakni, O., Hlila, R., Pour, A. B., Martín Martín, M., Maate, A., Maate, S., Muslim, A. M. and Hossain, M. S. (2022) Integrating Remote Sensing, GIS and *In-Situ* Data for Structural Mapping over a Part of the NW Rif Belt, Morocco. *Geocarto International*, **37**, 3265-3292. https://doi.org/10.1080/10106049.2020.1852611

[5] Chen, H. and Shi, Z. (2020) A Spatial-Temporal Attention-Based Method and a New Dataset for Remote Sensing Image Change Detection. *Remote Sensing*, **12**, 1662. https://doi.org/10.3390/rs12101662

[6] Chapman, G.R. and Brook, M. (1978) Chronostratigraphy of the Baringo Basin,

Kenya. *Geological Society*, *London*, *Special Publications*, **6**, 207-223. https://doi.org/10.1144/GSL.SP.1978.006.01.16

[7] Smith, M. and Mosley, P. (1993) Crustal Heterogeneity and Basement Influence on the Development of the Kenya Rift, East Africa. *Tectonics*, **12**, 591-606. https://doi.org/10.1029/92TC01710

[8] Bosworth, W., Lambiase, J. and Keisler, R. (1986) A New Look at Gregory's Rift: The Structural Style of Continental Rifting. *EOS Transactions*, **67**, 577-583. https://doi.org/10.1029/EO067i029p00577

[9] Bosworth, W. (1987) Off-Axis Volcanism in the Gregory Rift, East Africa: Implications for Models of Continental Rifting. *Geology*, **15**, 397-400. https://doi.org/10.1130/0091-7613(1987)15<397:OVITGR>2.0.CO;2

[10] Dunkley, P., Smith, M., Allen, D.J. and Darling, W.G. (1993) The Geothermal Activity and Geology of the Northern Sector of the Kenya Rift Valley. British Geological Survey, Research Report SC/98/1. https://nora.nerc.ac.uk/id/eprint/507920/1/SC_93_1_Report.pdf

[11] Joseph Martial, A., Ondoa Joseph, M., Jean Bosco, O., Jean, E. and Paul Kemeng, M. (2013) Utilisation des modèles numériques de terrain (MNT) SRTM pour la cartographie des linéaments structuraux : Application à l'Archéen de Mezesse à l'est de Sangmélima (Sud-Cameroun). *Geo-Eco-Trop*: *International Journal of Tropical Ecology and Geography*, **37**, 71-80. https://www.researchgate.net/publication/286306846_Application_of_MNT_SRTM_numeric_field_models_for_mapping_structural_lineaments_Application_to_the_Mezesse_Archean_East_of_Sangmelima_South_Cameroon

[12] Zeng, H., Xie, Z., Zhang, J., Zhu, Y., Zhao, F., Yang, S. and Zhao, X. (2021) A Methodology for Producing Realistic Hill-Shading Map Based on Shaded Relief Map, Digital Orthophotographic Map Fusion and IHS Transformation. *Annals of GIS*, **27**, 371-382. https://doi.org/10.1080/19475683.2021.1921026

[13] Maguire, D.J., Rhind, D.W. and Goodchild, M.F. (1991) Geographical Information Systems: Principles and Applications. Wiley, Hoboken.